Widely Tunable 1030 nm Gallium Arsenide Sampled Grating Distributed Bragg Reflector Lasers and Photonic Integrated Circuits

Paul Verrinder[1], Lei Wang[1], Fengqiao Sang[1], Victoria Rosborough[1], Guangning Yang[2], Mark Stephen[2], Larry Coldren[1], Jonathan Klamkin[1]

[1]Electrical and Computer Engineering Department, University of California, Santa Barbara, CA 93106 USA
[2]NASA Goddard Space Flight Center, Greenbelt, MD 20771 USA
pverrinder@ucsb.edu

Abstract: A widely tunable 1030 nm gallium arsenide laser with an integrated semiconductor optical amplifier was demonstrated. Continuous tuning across 22.2 nm and up to 70 mW output power was achieved. © 2022 The Authors

1. Introduction

The ability to easily tune the output wavelength of a laser is important for a variety of applications ranging from fiber telecom systems to free space communications and Lidar [1, 2]. In wavelength division multiplexing (WDM) systems, for example, the role previously filled by multiple standalone distributed Bragg reflector (DBR) lasers or distributed feedback (DFB) lasers can be reduced to a single wavelength tunable laser. Lidar systems can take advantage of this wavelength agility to accomplish beam steering by combining a tunable laser with diffractive grating elements. The laser and photonic integrated circuit (PIC) platform presented here are realized on gallium arsenide (GaAs) and with a nominal target center wavelength of 1030 nm. The sampled grating distributed Bragg reflector (SGDBR) laser architecture enables wide tuning range. The 10xx nm wavelength regime is of interest for a variety of applications including airborne Lidar (the target application), industrial, and biomedical [3, 4]. PIC technology enables a significant reduction in overall system cost, size, weight, and power (CSWaP) compared to currently deployed architectures for 1030 nm Lidar [4-6]. This is critical for space and airborne applications. Tunable lasers near 970 nm have been demonstrated on GaAs [7], however, the majority of commercially available tunable lasers at 1030 nm are external cavity lasers rather than monolithically integrated devices. Similar to indium phosphide (InP) for 1550 nm applications [8], the GaAs platform utilized here and described in [9] possesses the ability to integrate active and passive elements such as lasers, semiconductor optical amplifiers (SOA), modulators, photodetectors, couplers, and optical filters. The SGDBR laser demonstrates 22.2 nm of continuous tuning and up to 70 mW output with an integrated SOA.

2. Device Design and Fabrication

Figure 1(a) shows a sideview schematic of a four section SGDBR laser, with gain, front and back mirrors, and phase sections. Optical gain for the laser is provided by the multi-quantum well (MQW) gain region, consisting of three 5 nm thick indium gallium arsenide ($In_xGa_{1-x}As$) quantum wells (QWs) with $x = 0.271$, surrounded by gallium arsenide phosphide ($Ga_{1-x}AsP_x$) barriers with $x = 0.1$, to provide strain compensation. The MQW layers are surrounded by GaAs waveguide layers, and aluminum gallium arsenide (AlGaAs) separate confinement heterostructures (SCH). Integration of the active QW regions with the passive mirror and phase sections is accomplished by selectively removing the QW layers in the passive sections and regrowing the upper cladding layers by metalorganic chemical vapor deposition (MOCVD) after etching gratings for the front and back mirrors. Gratings for the SGDBR mirrors are patterned on the GaAs waveguide layer using electron beam lithography (EBL), and designed with a pitch of 157 nm for a Bragg wavelength of 1032.8 nm. The gratings are etched to a depth of 35 nm using inductively coupled plasma (ICP) etching with chlorine (Cl_2) and nitrogen (N_2) gas. The front and back mirrors are designed with different reflectivity spectra to exploit the Vernier effect for wide tuning.

This fabrication process was used to fabricate multiple lasers on a single die as shown in Fig. 1(b). Some of the fabricated lasers are simple four-section SGDBRs and some incorporate an SOA at the output after the front mirror for increased optical power. These devices are shown in the top-view microscope images in Figs. 1(d) and 1(e), respectively. In this paper we demonstrate results from the two devices shown in Figs. 1(d-e); one without an SOA and one with SOA. In both cases the length of the gain section is 500 μm, and for the amplified device, the length of

the SOA is 500 µm. After fabrication, individual lasers were cleaved out from the chip, anti-reflection (AR) coating was applied to the front and back facets, and the chip was mounted and wire bonded to a carrier as shown in Fig. 1(c).

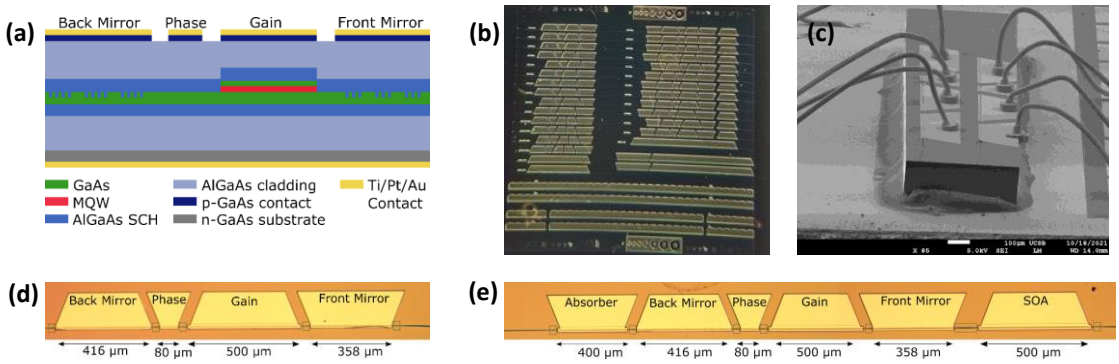

Fig. 1. (a) Side-view schematic of four section SGDBR laser, (b) plan-view microscope image of fabricated die, (c) SEM image of laser chip mounted and wirebonded to a carrier, (d) (e) top-view microscope image of fabricated laser without SOA, and with SOA, respectively.

3. Laser Performance and Characterization

Optical output power was measured by sweeping the current applied to the gain section of the laser and coupling the output to an integrating sphere. The continuous wave (CW) light-current (LI) characteristics are shown in Fig. 2(a) – the blue curve is for the laser without amplification, and the red curve represents the laser with an integrated SOA at the output biased at 100 mA. These devices can easily achieve 35 mW output power without amplification and greater than 70 mW with the SOA. Figure 2(b) shows SOA gain vs. total output power for 4 different current injection levels in the SOA, demonstrating over 25 dB of gain before saturation when the SOA is biased with 100 mA. The output from the laser was coupled to a lensed fiber and connected to an optical spectrum analyzer (OSA) to measure the output spectrum of the device. Figure 2(c) shows the free-running laser spectrum (i.e. current only applied to gain section, without mirror tuning) when the laser gain section is biased at 100 mA CW, demonstrating a peak wavelength of 1031.8 nm, and side-mode suppression ratio (SMSR) of 35 dB.

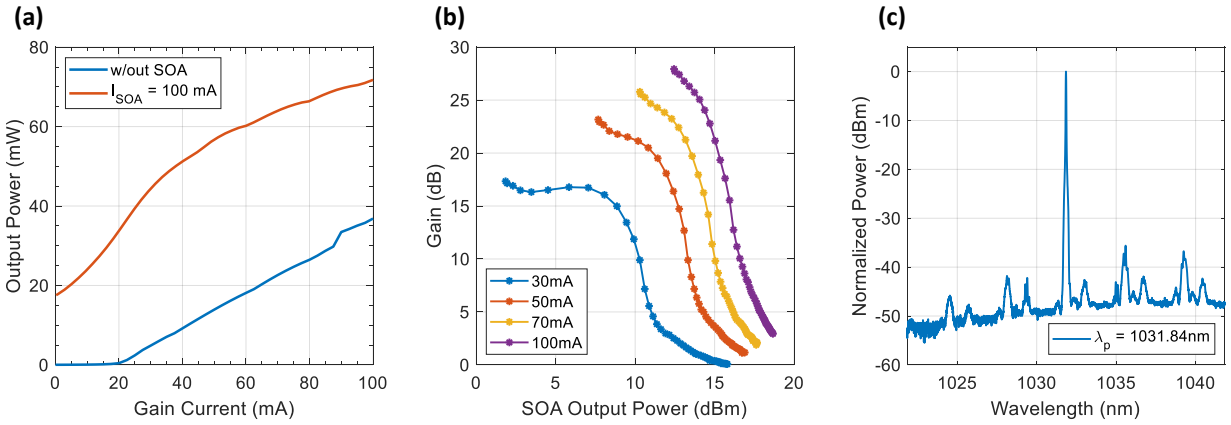

Fig. 2. (a) Optical power vs. current for laser without SOA (in blue) and laser with SOA (in red), (b) SOA gain vs. output power for varying SOA current levels, and (c) laser output spectrum without mirror tuning.

Tuning of the peak wavelength is accomplished by injecting current into the mirror and phase sections of the device. The injected current changes the index of refraction in that section, which shifts the peak of the reflectivity spectra and, therefore, the lasing wavelength. Tuning one mirror at a time will shift the output wavelength to the various available Vernier modes; this is shown in Fig. 3(a) where the spectra for 8 distinct Vernier modes are overlaid on a single plot to demonstrate a total tuning range of 22.2 nm (from 1026.1 nm to 1048.3 nm), with 30 dB SMSR at each

Vernier mode. Wavelengths between the peaks in Fig. 3(a) can be accessed by tuning both mirrors simultaneously, which shifts the peak continuously rather than hopping to adjacent Vernier modes. Figure 3(b) shows a contour plot for this laser, which was generated by tuning the front and back mirrors over every point from 0-150 mA to create a 150x150 grid of wavelength points as a function of mirror current. Figure 3(c) shows a contour plot of the SMSR associated with each point in Fig. 3(b). Tuning of the laser's phase section shifts the position of the cavity modes and, in conjunction with mirror tuning, can be used to avoid cavity mode hops as the laser is tuned from one Vernier mode to another. It should be noted that the SMSR contour plot in Fig. 3(c) was generated without any phase section tuning, and the very low SMSR data points in the plot are a result of mode hopping behavior. With fine tuning of the cavity modes, continuous mode-hop free tuning is possible with greater than 25 dB SMSR across the entire 22.2 nm range.

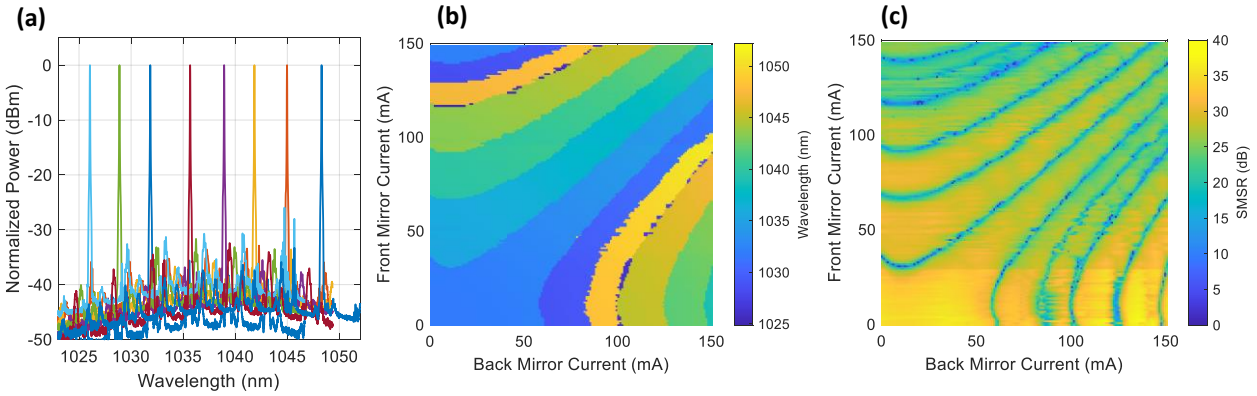

Fig. 3. (a) Overlaid lasing spectra showing Vernier mode positions. (b) Wavelength contour plot, and (c) SMSR contour plot

4. Conclusion

A widely tunable SGDBR laser on a GaAs PIC platform has been successfully demonstrated for operation near 1030 nm. The device demonstrates continuous, mode-hop free tuning across 22.2 nm with 30 dB SMSR, and greater than 70 mW of CW output power with amplification.

Acknowledgements

This work was supported by the NASA ESTO Advance Component Technology program. A portion of this work was carried out in the UCSB Nanofabrication Facility

References

[1] L. A. Coldren, G. A. Fish, Y. Akulova, J. S. Barton, L. Johansson, and C. W. Coldren, "Tunable Semiconductor Lasers: A Tutorial," *J. Light. Technol.*, vol. 22, no. 1, pp. 193–202, 2004, doi: 10.1109/JLT.2003.822207.
[2] B. J. Isaac, B. Song, S. Pinna, L. A. Coldren, and J. Klamkin, "Indium Phosphide Photonic Integrated Circuit Transceiver for FMCW LiDAR," *IEEE J. Sel. Top. Quantum Electron.*, vol. 25, no. 6, pp. 1–7, 2019, doi: 10.1109/JSTQE.2019.2911420.
[3] R. Kawakami *et al.*, "Visualizing hippocampal neurons with in vivo two-photon microscopy using a 1030 nm picosecond pulse laser," *Sci. Rep.*, vol. 3, pp. 1–7, 2013, doi: 10.1038/srep01014.
[4] A.W.Yu et al., "A 16-beam non-scanning swath mapping laser altimeter instrument" in Proc. SPIE LASE, San Francisco, CA, USA, 2013
[5] M. A. Krainak *et al.*, "Laser transceivers for future NASA missions," in Proc. SPIE Defense, Security, and Sensing, Baltimore, MD, USA, 2012
[6] A. W. Yu *et al.*, "Orbiting and in-situ lidars for earth and planetary applications," *IEEE J. Sel. Top. Appl. Earth Obs. Remote Sens.*, vol. 14, pp. 8999–9011, 2021, doi: 10.1109/JSTARS.2021.3103929.
[7] M. Tawfieq, H. Wenzel, P. Della Casa, O. Brox, A. Ginolas, P. Ressel, D. Feise, A. Knigge, M. Weyers, B. Sumpf, and G. Tränkle, "High-power sampled-grating-based master oscillator power amplifier system with 23.5 nm wavelength tuning around 970 nm," *Appl. Opt.,* vol. 57, no. 29, pp. 8680-8685, 2018
[8] H. Zhao *et al.*, "Indium Phosphide Photonic Integrated Circuits for Free Space Optical Links," *IEEE J. Sel. Top. Quantum Electron.*, vol. 24, no. 6, pp. 1–6, 2018, doi: 10.1109/JSTQE.2018.2866677.
[9] P. Verrinder *et al.*, "Gallium Arsenide Photonic Integrated Circuit Platform for Tunable Laser Applications," *IEEE J. Sel. Top. Quantum Electron.*, vol. 28, no. 1, 2022, doi: 10.1109/JSTQE.2021.3086074.